Practical controller design for ultra-precision positioning of stages with a pneumatic artificial muscle actuator

2017 IOP Conf. Ser.: Mater. Sci. Eng. 210 012056

(http://iopscience.iop.org/1757-899X/210/1/012056)

Practical controller design for ultra-precision positioning of stages with a pneumatic artificial muscle actuator

T F Tang and S H Chong
Centre for Robotics and Industrial Automation, Faculty of Electrical Engineering, Universiti Teknikal Malaysia Melaka, Hang Tuah Jaya, 76100 Durian Tunggal, Melaka, Malaysia.

E-mail: horng@utem.edu.my

Abstract. This paper presents a practical controller design method for ultra-precision positioning of pneumatic artificial muscle actuator stages. Pneumatic artificial muscle (PAM) actuators are safe to use and have numerous advantages which have brought these actuators to wide applications. However, PAM exhibits strong non-linear characteristics, and these limitations lead to low controllability and limit its application. In practice, the non-linear characteristics of PAM mechanism are difficult to be precisely modeled, and time consuming to model them accurately. The purpose of the present study is to clarify a practical controller design method that emphasizes a simple design procedure that does not acquire plants parameters modeling, and yet is able to demonstrate ultra-precision positioning performance for a PAM driven stage. The practical control approach adopts continuous motion nominal characteristic trajectory following (CM NCTF) control as the feedback controller. The constructed PAM driven stage is in low damping characteristic and causes severe residual vibration that deteriorates motion accuracy of the system. Therefore, the idea to increase the damping characteristic by having an acceleration feedback compensation to the plant has been proposed. The effectiveness of the proposed controller was verified experimentally and compared with a classical PI controller in point-to-point motion. The experiment results proved that the CM NCTF controller demonstrates better positioning performance in smaller motion error than the PI controller. Overall, the CM NCTF controller has successfully to reduce motion error to 3μm, which is 88.7% smaller than the PI controller.

1. Introduction

Nowadays, the human sciences and technology are getting more advanced and widespread. The usage and number of robotic and automation applications are increasing due to the development of advanced technologies. Linear positioning systems are the fundamental mechanisms that play important roles in the industrial machines such as machine tools, semiconductor manufacturing system and robotics. For robotic applications, the system performance is characterized by constraints such as power to weight ratios, response rate, physical size, speed of motion, realiability, controllability, compliance, and cost [1]. Those applications have required an actuation system as function in providing force, torque or mechanical motion, in order to drive the motion of the system. Typically, a robot system is designed extremely stiff and built with strong joint actuators, in order to overcome threshold friction, position-dependent gravity and payloads [2]. However, the robot systems are high cost and high energy consumption due to their heavy construction. Besides, their large strength are too dangerous to use in environment, where they are operating by human.

Pneumatic actuators are traditional actuators and have numerous advantages, such as simple structure, low component cost, high power-to-weight ratio, ease of maintenance, high safety and many more. Therefore, these advantages have led to the development of a novel actuator, namely McKibben pneumatic artificial muscle (PAM), which was originally inverted in the 1950s by the American physician, J. L. McKibben. PAM is a mechanical apparatus that duplicates the behaviour of skeletal muscle, where it contracts and generates a pulling force in a non-linear way once it is activated [3]. This PAM consists of an inflatable rubber tube sheathed by a braided mesh. When pressurized, the rubber tube tends to increase in volume. Due to the non-extensibility of the thread in the braided mesh, it restricts the rubber tube to expand in radius but shortens axially instead [4]. The pneumatic energy in the pressurized air is thus transformed into mechanical work. Since PAM only has one active action which is contraction, thus it must always be operated in antagonistic actions. These antagonistic actions can either involve two active PAMs or a single active PAM coupled to a spring.

The physical configuration of PAM has variable-stiffness spring like characteristics, and it is very light weight compared to other types of actuators [5]. It is a promising actuator in robotics since its driving force is large despite its light weight. The power-to-weight ratio of PAM is about five times higher than the ratio of electric motors or hydraulic actuators. Besides, PAM can exert the force about ten times of a comparably sized pneumatic cylinder [6]. Thus, PAM actuators are safe to use and have numerous advantages which have brought these actuators to wide applications, especially in rehabilitation and welfare devices. For example, they have been applied in the power assist devices [7–10], robotics [11], medical applications [12] and industrial machinery [13]. However, the PAM is exhibits strong non-linear characteristics [14], low damping ability, hysteresis [15] and creep phenomenon [16]. These limitations lead to a low controllability and a high difficulty in achieving the precision system control and limit its application. Furthermore, the air compressibility and lack of damping ability of PAM mechanism causes dynamic delay to the pressure response, which will results in oscillatory motion. As a result, it is not easy to realize the motion with high accuracy and high speed.

An enhancement of the PAM in positioning accuracy is desirable due to its advantages, and then extend its applications in the precision positioning system. For example, the precise motion of PAM allows nursing care robot to provide disabled people with delicate supports such as injection, rehabilitation support and transfer assist. In the industrial, the precision control of PAM allows to create a precise assembly robot which is powerful and lightweight as well as safer to assemblers who work with the robots. As compared with hydraulic and pneumatic cylinders, PAM has superior characteristics when applied to welfare devices, thus the development of PAM with precision motion could be a promising advancement for future neurosurgical robots [17].

In recent years, numerous control methods have been proposed to control the motion of the PAM mechanisms. These methods can be classified in three categories which are classical proportional-integral-derivative (PID) control, non-linear model-based control and intelligent control. Classical PID control is the most popular ones and often used for positioning systems. The PID control is easy to design, but it is not robust to the change of parameters and insufficiently to compensate for the non-linearity of the PAM mechanism which lead to poor accuracy. Caldwell *et al.* [18] proposed a feed-forward PID controller for controlling a pneumatic muscle. The result showed that the performance was quite sensitive to errors in the feed-forward term, due to fluctuations of supply pressure, temperature and muscle characteristics. In [19–21], the authors reported that the motion accuracy produced by classical PID controller is 0.1° for rotational positioning. For linear PAM mechanism, the highest positioning accuracy produced by a PID controller is 200 μm [19]. The classical PID controller does not solve the hysteresis problem.

Non-linear model-based control is a popular approach that applied to the PAM mechanisms. Due to inaccurate modeling, the positioning accuracy for the PAM mechanisms is on the order of a micrometer [22]. Sliding mode controller (SMC) had been applied to the PAM mechanisms in [23, 24]. However, the simulation results were presented only for the effectiveness of the strategy. Tondu and Lopez proposed a sliding mode controller using a non-linear length-tension model of the PAMs [25]. Besides, Li *et al.* [26]

proposed a non-linear dynamic force model that generated by a PAM, which was achieved 6 μm as the highest positioning accuracy. Different modified non-linear model-based controllers have been proposed in the literature, but the controllers were managed to compensate the positioning error on the order of a micrometer due to the inaccurate modeling. In practice, the non-linear characteristics of the PAM mechanism are difficult to be precisely modeled, and time consuming to model them accurately. As a result, it is difficult to design and impracticable for the engineers who are unfamiliar and insufficient knowledge of the control theory with the controller design that requires the mechanism modeling. Intelligent control has also been widely used for the PAM mechanism. Hesselroth *et al.* [27] proposed a Kohonen-type neural network learning algorithm to control a five-joint pneumatic robot arm and gripper through feedback from two video cameras as visual observation of real and desired end-effector position. However,the Kohonen neural network algorithm is compressing a large data set, and the learning sessions are very time consuming. Therefore, the system has limited practical applicability. Chan *et al.* [28] proposed a fuzzy PD+I learning control that has good results with accurate positioning of the pneumatic muscle after a few seconds of operation. However, some limitations still exist because the necessary time for learning is quite long and the controller output functions properly after about 30 to 45 seconds according to the input signal. Furthermore, Ahn *et al.* [29] proposed an intelligent switching control method to adjust the gains of PID controller using neural networks. This method shows the most accurate positioning result with a rotational positioning error of 0.05° for the intelligent control of the PAM mechanism. The neural network controller with learning capabilities provide an efficient method to satisfy the positioning requirements. However, intelligent control has a complex controller design and no general systematic approach to choose the neural control structure, which require sufficient knowledge of the intelligent algorithm when it applied for the PAM mechanisms. Regardless the mechanical complexity, the control design method should still be easy and straightforward. Thus, a practical controller, which has a simple design procedure and capable to demonstrate high robustness with the changes of plant parameters and positioning accuracy performance is desired to overcome the stated problems. This is always the solution that needed in the industry. As mentioned before, the PAM need to be operated in antagonistic actions. In this research, a PAM mechanism is constructed with a mover that is located in the middle of two PAMs in an opposing pair configuration. The purpose of the present study is to clarify a practical controller design method that emphasizes a simple design procedure that does not acquire plants parameters modeling, and yet is able to demonstrate ultra-precision positioning performance for a PAM driven stage. The effectiveness of the proposed controller is verified experimentally and compared with a classical PI controller in point-to-point (PTP) motion. The rest of this paper is organized as follows. Section 2 describes the experimental setup and provides a brief review of the characteristic of the PAM driven stage. Section 3 introduces the CM NCTF control concept and the proposed design procedure. In Section 4, the PTP positioning control performances of the CM NCTF controller are evaluated and compared with the PI controller. The conclusion of the present study is remarked in Section 5.

2. Characteristics of PAM driven stage

2.1. Experimental setup

An experimental setup is designed and constructed as a linear antagonistic structure using two PAMs and a mover is located in between the two PAMs in a horizontal motion, as shown in Figure 1. The two PAMs (FESTO DMSP-10-150N-RM-CM) generate pulling forces to push and pull the 2 kg mover along the horizontal moving direction in a maximum working range of ±3.2 mm. As an input source, air is injected from the pressure supply with a pressure of 0.5 MPa and controlled by a 5-port 3-way proportional servo valve (FESTO MPYE-5-1/8LF-010-B). The pressures in the two PAMs are measured using two pressure sensors (SMC PSE540A-01) with the resolution of 0.0012 MPa, which are not used as feedback sensors for control but are instead used to observe the air pressures. A linear encoder with the resolution of 0.1 μm is used as a single feedback sensor in this mechanism to measure the displacement of the mover. For the signals processing, a data

acquisition unit is used to interface with a host computer that installed MATLAB/Simulink software. The sampling time, T_S is 0.1 ms.

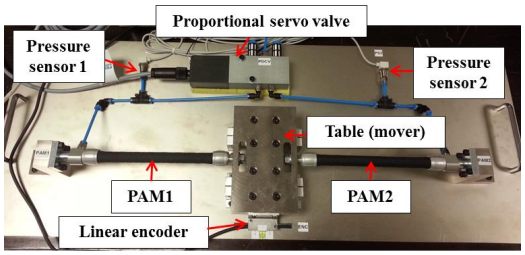

Figure 1. PAM driven stage.

2.2. Static relationships

Based on the experimental open-loop responses, the static relationships between input voltage, pressures of PAM1 and PAM2, and displacement of the mover are summarized. Figure 2 presents the static relationship between input voltage and pressures of PAM1 and PAM2; the static relationship between input voltage and displacement. The result shows that the system is high non-linearities.

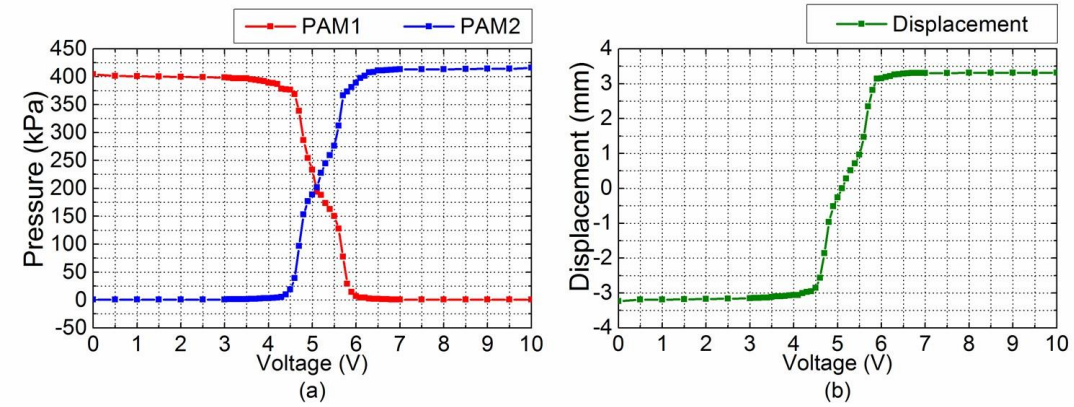

Figure 2. The static relationships between (a) input voltage and pressures of PAM1 and PAM2, and (b) input voltage and displacement.

As shown in Figure 2(a), a small change of an input voltage within 4.5 V to 5.8 V, it gives a large different in the pressure of both PAMs. However, the pressures from 0 V to 3 V and 7 V to 10 V have slight changes with respect to the large changes of input voltage. The ratio of output pressure over input voltage is very small. Also, the working range is saturated around ±3.2 mm as can be found in Figure 2(b). These are due to the antagonistic structure of PAM mechanism. The relaxed PAM becomes stiff when it has been pulled over the elasticity limit, and the contractile force could not against it with the supplied pressure. Besides, the result of the displacement is non-linear between the contraction of the PAM1 and PAM2 due to the hysteresis and non-linear friction force. The maximum pressure of the contracted PAM is about 390 kPa rather than 500 kPa (supply pressure), due to the losses caused by the friction inside the tubing and leakage from the servo valve when the pressurized air transferred from the compressor to the PAM.

2.3. Dynamic model

Figure 3 shows the free body diagram of PAM mechanism. The initial position of the mover is in the middle position, 0 mm. When the contraction of PAM1, the mover is moving to the left direction with negative value of displacement. The displacement of the mover is then considered as positive value when PAM2 is contracting. The PAM is stated as variable-stiffness spring-like characteristics due to its physical structure. The motion equation of the PAM mechanism can be written as Equation 1.

$$M\ddot{x} + B\dot{x} + Kx = F_2 - F_1 - F_{friction} \quad (1)$$

Where M is the mass of the stage, B is the damping coefficient, and K is the spring coefficient. The generated forces of PAM1 and PAM2 are stated as F_2 and F_1, respectively. $F_{friction}$ represents the friction force between the stage and the linear guide.

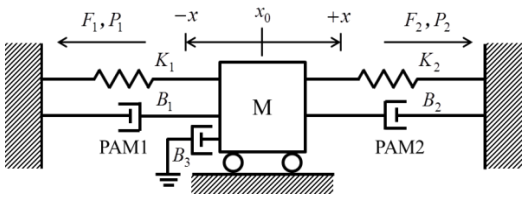

Figure 3. Free body diagram of PAM mechanism.

3. Controller design

3.1. CM NCTF control structure

Continuous Motion Nominal Characteristic Trajectory Following (CM NCTF) controller is an improved control strategy of Nominal Characteristic Trajectory Following (NCTF). The CM NCTF controller has been modified to improve the motion control performances in tracking motion and contouring motion, while it is maintaining point-to-point (PTP) positioning that offered by the NCTF controller [30]. The main contribution of the CM NCTF controller is emphasizes a simple and easy design procedure, in order to achieve the promising results in both positioning motion and continuous motion controls. As an advantage, this controller does not require an exact model of the plant and its parameters, which makes it easy to design, understand and adjust. This makes it is user-friendly to engineers who are lack of control theory knowledge to handle.

Figure 4 shows the structure of the CM NCTF control system. The CM NCTF controller consists of two main parts which are a Nominal Characteristic Trajectory (NCT) and PIcompensator. The NCT is the reference motion trajectory of the control system that used to restrict the motion of the mechanism along the trajectory, and it is expressed on phase plane. The NCT is constructed from the actual responses such as displacement and velocity responses of a mechanism in open-loop condition, which the characteristic of the mechanism that influenced by the friction and saturation effects are captured. The determined NCT represents the deceleration motion of the mechanism in positioning, which it is significantly affect the positioning performance. Subsequently, the PI compensator controls the object motion to follow the determined NCT, and further end the motion at the origin of the phase plane. The PI compensator works for reduction of the difference between the NCT and the actual motion when the difference is increased by the disturbance forces and mechanism characteristic changes. The PI compensator is designed based on the stability of the system.

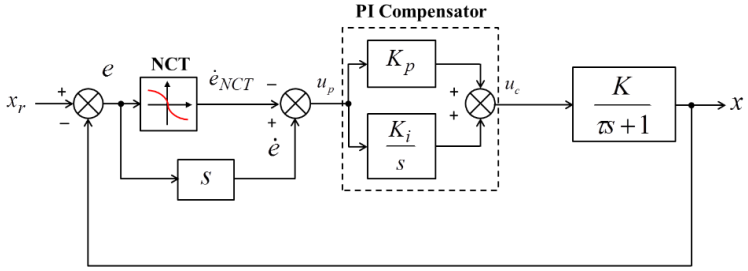

Figure 4. Structure of the CM NCTF control system.

The conventional CM NCTF controller has demonstrated a higher positioning performances for electric-motor driven mechanism [31], non-contact mechanism and contact mechanism [32]. However, the response of the control system exhibits oscillation in the steady-state response when applied in the PAM mechanism. This is due to low damping characteristic of the constructed PAM driven stage causes severe residual vibration that deteriorates motion accuracy of the system. Therefore, the idea to increase the damping characteristic by having an acceleration feedback compensation to the plant has been proposed. An acceleration feedback is then added to increase the damping effect of the PAM mechanism, in order to eliminate the oscillation and achieve better accuracy. Figure 5 presents the structure of CM NCTF control system with the acceleration feedback.

$$G_{po}(s) = \frac{K}{KK_a s^2 + \tau s + 1}$$

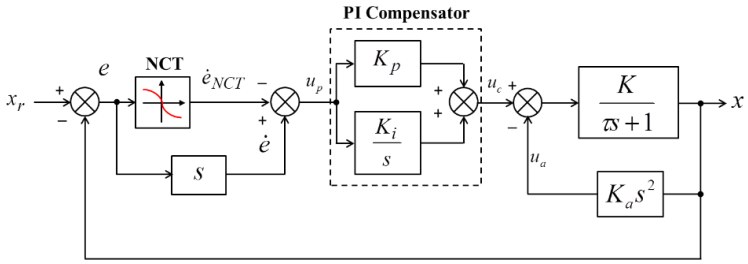

Figure 5. Structure of the CM NCTF control system with the acceleration feedback.

The linearized open-loop transfer function of the PAM mechanism, G_{pon}can be obtained as shown in Equation 2. The plant model is considered as second-order system. Thus, the acceleration feedback is expected to be increasing the damping effect and enhanced the accuracy effectively.

3.2. Design procedure

The main consideration of the CM NCTF control design procedure is simple and easy to design, which the detailed dynamic model and its exact parameters are not required. In this paper, the CM NCTF with an acceleration feedback is designed and applied in the PAM driven stage. Generally, the design procedure of the controller is comprised four major steps:

(1) Determination of open-loop responses.
The mechanism is executed with an open-loop step input, and its displacement and velocity are then measured. Wahyudi *et al.* [33] stated that the amplitude of input is chosen 80% of the rated input to the actuator, which the overall system dynamics are included in the measured responses. Thus, a step input of 4 V is used to measure the PAM mechanism. Figure 6 presents the open-loop responses of the PAM mechanism.

(2) Construction of NCT.
The NCT is constructed on the phase plane using the displacement and velocity of the mechanism during deceleration. The obtained responses in the open-loop condition during the deceleration are directly selected to construct the NCT, and without further do the mathematics derivation for the dynamics of the mechanism. The NCT works as virtual reference error rate, with the inclination at origin is referred as β. Based on the obtained responses, the NCT can be constructed as shown in Figure 7. The inclination at origin, β in this case is 208 s^{-1}.

(3) Design of PI compensator.
The PI compensator is designed based on the open-loop responses and NCT information. In order to consider the real characteristic of the mechanism in designing the PI compensator, a practical stability limit is determined as the margin in selecting the PI gains that bounded under the stable region of the actual mechanism. The discussion about the determination of practical stability limit and choice of the design parameters could be found in Section 3.3.

(4) Determination of acceleration gain.
The acceleration gain, K_a is determined experimentally for sufficient damping characteristics using a mechanism that embedded the CM NCTF controller with an optimum PI compensator. The fined-tuned K_a is 6×10^{-6} Vs^2/mm.

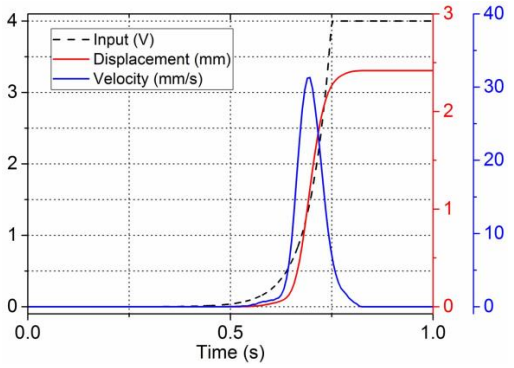

Figure 6. Open-loop responses of the PAM mechanism.

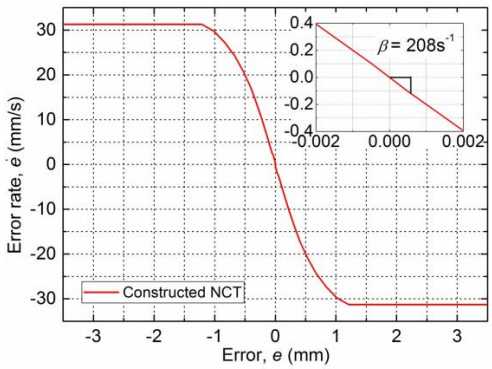

Figure 7. Constructed NCT from open-loop responses.

The practical stability limit is used to choose the PI gains within the stable operation region which can be easily calculated independently of the actual mechanism characteristic. Few parameters have to determine first before find the practical stability limit. In order to estimate the parameters of plant model, the normalized of the open-loop step responses of the PAM mechanism under different step input voltages are measured. Figure 8 and Figure 9 show normalized open-loop step responses and its average step response, and an estimated model respectively.

$$G_{closedloop}(s) = \frac{2\zeta\omega_n s + \omega_n^2}{s^2 + 2\zeta\omega_n s + \omega_n^2} = \frac{KK_p s^2 + (\beta KK_p + KK_i)\, s + \beta KK_i}{(KK_p + \tau)\left[s^2 + \left(\frac{\beta KK_p + KK_i + 1}{KK_p + \tau}\right) s + \left(\frac{\beta KK_i}{KK_p + \tau}\right)\right]} \quad (2)$$

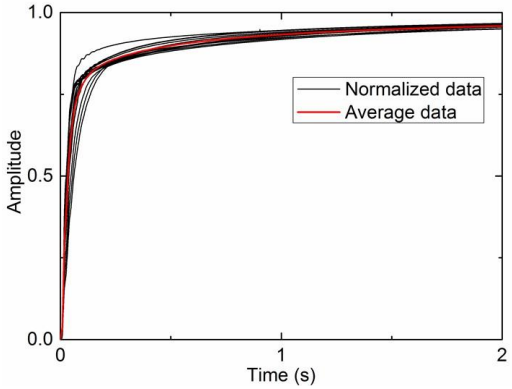

Figure 8. Normalized open-loop step responses and an average response.

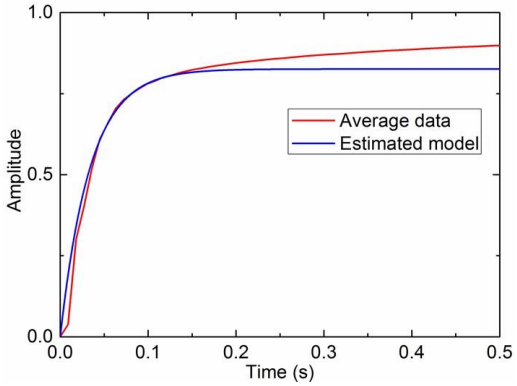

Figure 9. The average response and an estimated first-order model.

An estimated first-order model of the mechanism is based on a linear macrodynamic model expressed as:

$$\zeta_{practical} = \frac{\beta^2 K K_{pu} + K K_{pu}\omega_n^2 + \tau\omega_n^2 + \beta}{2\omega_n K K_{pu}\beta + 2\omega_n \tau\beta} \tag{3}$$

$$K_p = \frac{\tau\omega_n^2 + \beta - 2\zeta\omega_n\beta\tau}{2\zeta\omega_n\beta K - \beta^2 K - K\omega_n^2} \tag{4}$$

$$K_i = \frac{K K_p\omega_n^2 + \tau\omega_n^2}{\beta K} \tag{5}$$

where K is the system gain and τ is the time constant. The creep phenomenon is happened after the final state, which the estimated linear model could not model it. However, the estimated model is sufficient to represent the characteristic of PAM driven stage. Based on the CM NCTF control system as shown in Figure 4, the closed-loop transfer function is expressed as second- order system in Equation 4. The determined inclination at origin, β is 208 s^{-1} from the NCT.

The practical stability limit of the actual mechanism is found by driving the mechanism with the CM NCTF controller using only the proportional element. The value of proportional gain is increased until continuous oscillations which indicates the existence of instability. However, the continuous oscillations is not applicable to the PAM mechanism, due to it is a first-order system. Thus, the maximum proportional gain is decided when the PAM mechanism is vibrating. The maximum proportional gain is referred as an actual ultimate proportional gain, K_{pu} (0.0018Vs/mm in the case of the PAM mechanism). Based on Equation 4, the practical stability limit, $\zeta_{practical}$, proportional gain, K_p and integral gain K_i are derived as follows:

$$G_{po}(s) = \frac{K}{\tau s + 1} = \frac{0.826}{0.034s + 1}$$

For the maximum natural frequency, ωn of the PAM mechanism, it is determined through the open-loop frequency response and the break frequency is 17.7 rad/s at -3 dB. Therefore, the range of ωn in the practical stability limit is set from 1 rad/s to 16 rad/s, which the limit is slightly lower than the break frequency. By varying the ωn, the practical stability limit is constructed using Equation 6. The points are defined by ζ and ωnTs (Ts = 0.0001 s) as presented in Figure 10. The PI compensator is selected within the stable region. From the stability limit (safety margin), the PI compensator is choose 90% of the value of $\zeta practical$, which is 10% of safety margin.

Four points are selected to verify the positioning performances as shown in Figure 11. Table 1 details the parameters of the selected PI compensator. Step input of 2 mm is used as reference input for the PAM mechanism. Figure 12 shows the positioning performances of P1, P2, P3 and P4. P3 is the optimum PI parameters (Kp = 0.0142 Vs/mm and Ki = 0.0384 Vs^2/mm) which demonstrates faster transient response compared to P1 and P2. However, P1 encounter vibration during the transient because it is too fast for the PAM mechanism to react the 2 mm step amplitude. The problem is not occurred in the smaller working range. This is the reason of choosing 2 mm as the reference input rather than 1 mm or smaller working range. Overall, the design procedure of the CM NCTF controller has shown the simplicity and straightforward in determine the required parameters which can be measured directly from the mechanism.

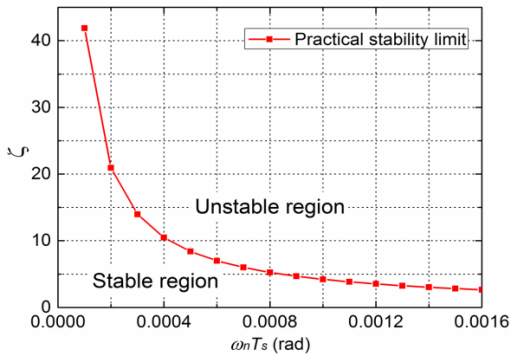

Figure 10. Relationship between stability, ζ and ωn, and practical stability limit.

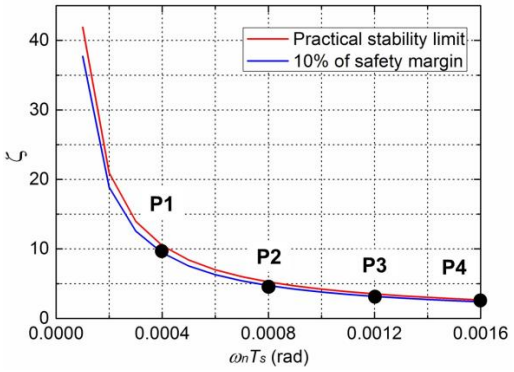

Figure 11. Four different points of PI compensator on 10% of safety

Table 1. Parameters of the selected PI compensator.

	ω_n (rad/s)	$\omega_n T_s$ (rad)	ζ	90% of ζ	K_p (Vs/mm)	K_i
P1	4	0.0004	10.478	9.4302	0.0143	0.0043
P2	8	0.0008	5.2534	4.7281	0.0143	0.0171
P3	12	0.0012	3.5183	3.1665	0.0142	0.0384
P4	16	0.0016	2.6556	2.3900	0.0142	0.0682

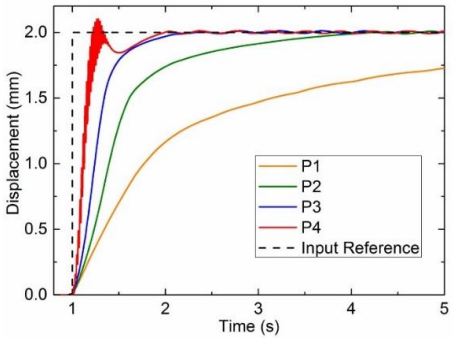

Figure 12. Positioning performances of P1, P2, P3 and P4.

4. Experimental result

In this section, different positioning performances are experimentally examined. The effectiveness of the CM NCTF controller is evaluated in comparison with the PI controller. The PID controller is not chosen instead of the PI controller because the PID controller does not show a significant improvement in the positioning performance for the PAM mechanism. The CM NCTF controller is designed through the procedure as shown in Section 3.2. The NCT shown in Figure 7 and controller parameters designed in Section 3.3 are used. The PI controller which is used to compare the CM NCTF controller is designed to have an optimum performance. The fine-tuned PI controller gains are Kp = 0.4 V/mm and Ki = 3.5 Vs/mm under a reference input of 2 mm. Figure 13, Figure 14 and Figure 15 present the PTP positioning performances comparison between the CM NCTF controller and the PI controller with 0.1 mm, 1 mm and 2 mm respectively.

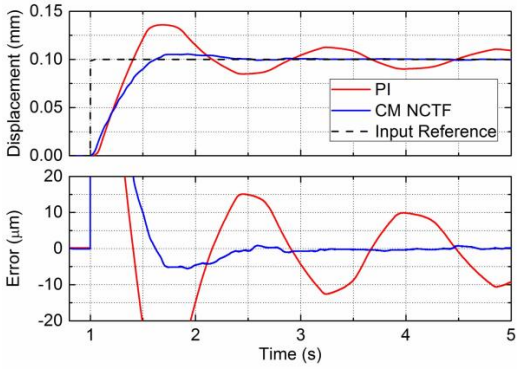

Figure 13. PTP positioning performance comparison in 0.1 mm between the CM NCTF controller and the PI controller.

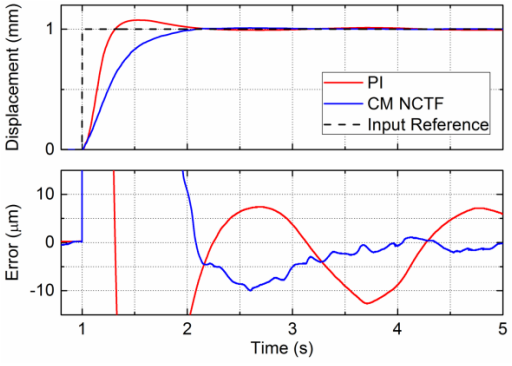

Figure 14. PTP positioning performance comparison in 1 mm between the CM NCTF controller and the PI controller.

The positioning result of the CM NCTF controller differ considerably to the PI controller. The result of both controllers is summarized in Table 2. The CM NCTF controller demonstrates a better positioning performance compared to PI controller. In overall, the CM NCTF controller has achieved the positioning accuracy within 3 µm of steady-state error. The CM NCTF controller also demonstrates the consistency of positioning accuracy in different step height.

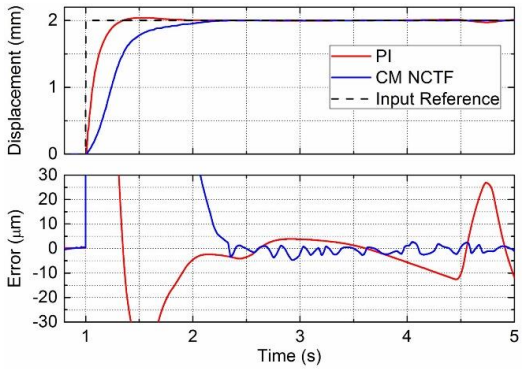

Figure 15. PTP positioning performance comparison in 2 mm between the CM NCTF controller and the PI controller.

In contrast to the PI controller, the CM NCTF controller shows 88.7% smaller steady-state error as an average. As observed from Table 2, the huge overshoot from the PI controller is increasing when the reference step input is reduced. By contrast, the CM NCTF controller exhibits smaller and acceptable overshoot than the PI controller in all the working range. However, the CM NCTF controller offers longer rise time and settling time as compared to the PI controller. This is due to the reference motion trajectory from the NCT and the characteristic of the CM NCTF controller. As aforementioned, the NCT is used to restrict the motion of the mechanism. Thus, it will help in reducing the overshoot, which is found lack in the PI controller. Overall, it can be concluded that, the PI controller is lack of adaptability to precision motion control in comparison with the CM NCTF controller.

Table 2. PTP positioning performances of the CM NCTF controller and the PI controller.

Step height	Performance index	PI controller	CM NCTF controller	Improvement
0.1 mm	Rise time	0.27 s	0.44 s	-
	Settling time	1.13 s	1.29 s	-
	Overshoot	35.90%	5.60%	84.40%
	Steady-state error	15.0 µm	1.1 µm	92.67%
1 mm	Rise time	0.19 s	0.56 s	-
	Settling time	0.98 s	1.08 s	-
	Overshoot	7.53%	1.00%	86.72%
	Steady-state error	12.7 µm	2.1 µm	83.46%
2 mm	Rise time	0.19 s	0.44 s	-

Settling time	0.58 s	1.34 s	-
Overshoot	2.04%	0.18%	91.18%
Steady-state error	26.9 µm	2.7 µm	89.96%

5. Conclusion

In the present paper, the CM NCTF controller was proposed as a practical controller design method for ultra-precision positioning. The CM NCTF controller was applied to the PAM driven stage for evaluation of its effectiveness. The controller structure and design procedure are simple and straightforward. The controller parameters were determined using the practical stability limit which makes the tuning procedure more practical than manual tuning. The PTP positioning performances with the CM NCTF controller were evaluated based on the experimental results. The performances with the CM NCTF controller were then compared with the PI controller. Overall, the results prove that the performances obtained using the CM NCTF controller is better than those obtained using the PI controller. The CM NCTF controller has successfully reduced the motion error to 3 µm, which is 88.7% smaller than the PI controller. Besides, the simplicity in design procedure of the CM NCTF controller showed the capability in performing high precision motion and promising results in positioning control. As the future work, the performance of the CM NCTF controller will improve in the transient response and evaluate in the tracking performance.

Acknowledgments

The authors would like to be obliged to Centre for Robotics and Industrial Automation, Faculty of Electrical Engineering, Universiti Teknikal Malaysia Melaka for providing the laboratory facilities and equipment support. This work is financially supported by the Fundamental Research Grant Project (FRGS/1/2016/TK08/FKE-CeRIA/F00308) and the scholarship of Skim Zamalah from Universiti Teknikal Malaysia Melaka.

References

[1] Caldwell D G, Medrano-Cerda G A and Goodwin M 1995 *IEEE Control Systems* **15** 40-8
[2] Smagt P van der, Groen F and Schulten K 1996 *Biological Cybernetics* **75** 433-40
[3] Sakthivelu V and Horng C S 2013 *IEEE Student Conf. on Research and Development* (Putrajaya: IEEE) 60-4
[4] Minh T V, Tjahjowidodo T, Ramon H and Van Brussel H 2010 Cascade position control of a single pneumatic artificial musclemass system with hysteresis compensation *Mechatronics* **20** 402-14
[5] Chou C -P and Hannaford B 1996 *IEEE Transactions on Robotics and Automation* **12** 90-102
[6] Festo 2010 Fluidic muscle DMSP/MAS Festo brochure https://www.festo.com/cat/de_de/data/doc_de/PDF/DE/DMSP-MAS_DE.PDF
[7] Hussain S, Xie S Q and Jamwal P K 2013 *IEEE Transactions Systems, Man, Cybernetics: Systems* **43** 655-65
[8] Noritsugu T, Takaiwa M and Sasaki D 2010 *Next-Generation Actuators Leading Breakthroughs* (London: Springer) 255-66

[9] Sugar T G, He J, Koeneman E J, Koeneman J B, Herman R, Huang H, Schultz R S, Herring D E, Wanberg J, Balasubramanian S, Swenson P and Ward J A 2007 *IEEE Transactions on Neural Systems and Rehabilitation Engineering* **15** 336-46

[10] Wong Z, Teng C and Chong Y Z 2012 *IEEE-EMBS Conf. on Biomedical Engineering and Sciences* (Langkawi: IEEE) 300-4
[11] Hosoda K, Takuma T, Nakamoto A and Hayashi S 2008 *Robotics and Autonomous Systems* **56** 46-53
[12] Chakravarthy S, Aditya K and Ghosal A 2013 *Proc. of the 1st Int. and 16th National Conf. on Machines and Mechanisms* (Roorkee: Indian Institute of Technology Roorkee) 339-45
[13] Zhu X, Tao G, Yao B and Cao J 2009 *IEEE Transactions on Control Systems Technology* **17** 576-88
[14] Wickramatunge K C and Leephakpreeda T 2010 *Int. J. of Engineering Science* **48** 188-98
[15] Vo-Minh T, Tjahjowidodo T, Ramon H, Van Brussel H 2011 *IEEE/ASME Transactions on Mechatronics* **16** 177-86
[16] Minh T V, Kamers B, Ramon H, Van Brussel H 2012 *Mechatronics* **22** pp 923-33
[17] Wang S and Sato K 2016 *Precision Engineering* **43** 448-61
[18] Caldwell D G, Medrano-Cerda G A and Goodwin M J 1993 *Proc. of IEEE Systems Man and Cybernetics Conf.* (Le Touquet: IEEE) 423-8
[19] Andrikopoulos G, Nikolakopoulos G and Manesis S 2013 *21st Mediterranean Conf. on Control and Automation* (Platanias-Chania, Crete: IEEE) 729-34
[20] Li X, He F, Hong X and Guan T 2011 *Applied Mechanics and Materials* **138-9** 273-8
[21] Pujana-Arrese A, Mendizabal A, Arenas J, Prestamero R and Landaluze J 2010 *Mechatronics* **20** 535-52
[22] Xing K, Xu Q, Huang J, Wang Y, He J and Wu J 2010 *IET Control Theory and Applications* **4** 2058-70
[23] Carbonell P, Jiang Z P and Repperger D W 2001 *Proc. of the IEEE Int. Conf. on Control Applications* (Mexico City: IEEE) 167-72
[24] Lilly J H and Liang Y 2005 *IEEE Transactions on Control Systems Technology* **13** 550-8
[25] Tondu B and Lopez P 2000 *IEEE Control Systems Magazine* **20** 15-38
[26] Li H, Kawashima K, Tadano K, Ganguly S and Nakano S 2013 *IEEE/ASME Transactions on Mechatronics* **18** 74-85
[27] Hesselroth T, Sarkar K, van der Smagt P P and Schulten K 1994 *IEEE Transactions on Systems, Man, and Cybernetics* **24** 28-38
[28] Chan S W, Lilly J H, Repperger D W and Berlin J E 2003 *The 12th IEEE Int. Conf. on Fuzzy Systems* 278-83
[29] Ahn K K, Thanh T D C and Ahn Y K 2005 *JSME Int. J. Series C* **48** 657-67
[30] Chong S -H and Sato K 2016 *IECON 2015 - 41st Annual Conf. of the IEEE Industrial Electronics Society* (Yokohama: IEEE) 4790-5
[31] Sato K and Maeda G J 2009 *Precision Engineering* **33** 175-86
[32] Chong S -H and Sato K 2010 *Precision Engineering* **34** 286-300
[33] Wahyudi, Sato K and Shimokohbe A 2001 *IEEE/ASME Int. Conf. on Advanced Intelligent Mechatronics* vol 2 (Como: IEEE) 843-8